A New Theory for the Atmospheric Energy Spectrum: Depth-Limited Temperature Anomalies at the Tropopause

R. Tulloch* **and K. S. Smith***

*Center for Atmosphere Ocean Science, Courant Institute of Mathematical Sciences, New York University, 251 Mercer Street, New York, NY 10012

Communicated by Andrew J. Majda, June 27, 2006

The horizontal spectra of atmospheric wind and temperature at the tropopause have a steep -3 slope at synoptic scales, but transition to $-5/3$ at wavelengths of order 500–1000 km [1]. Here we demonstrate that a model that assumes zero potential vorticity and constant stratification N over a finite depth H in the troposphere exhibits the same type of spectra. In this model temperature perturbations generated at the planetary scale excite a direct cascade of energy with a slope of -3 at large scales, $-5/3$ at small scales and a transition near horizontal wavenumber $k_t = f/NH$, where f is the Coriolis parameter. Ballpark atmospheric estimates for N, f and H give a transition wavenumber near that observed and numerical simulations of the new model verify the expected behavior. Despite its simplicity, the model is consistent with a number of perplexing features in the observations, and demonstrates that a complete theory for mesoscale dynamics must take temperature advection at boundaries into account.

In the 1970s NASA instrumented commercial Boeing 747 airliners to collect atmospheric data during their regular flights [1, 2] in an endeavor called the Global Atmospheric Sampling Program (GASP). The resulting dataset consists of thousands of flight tracks, a few hundred of which are over $10,000$ km long, collected over a four year period. Most flights occurred in the mid-latitudes and tropics, but span the full range of seasons. Because airliners travel at altitudes between 9 and 14 km, the data largely reflect the upper troposphere and lower stratosphere, near the tropopause. Atmospheric wavenumber spectra of horizontal wind and temperature computed from the GASP dataset by Nastrom and Gage [1, hereafter NG85], reprinted here in figure 1, show a distinct transition from a steep spectral slope of -3 at synoptic scales ($\sim$ 1000 to 3000 km) to a shallower slope of $-5/3$ at mesoscales ($\sim$ 10 to 500 km), with a fairly distinct transition centered at a horizontal wavelength of about 600 km. Understanding the source and structure of this spectrum has posed a puzzle in atmospheric science for the past 20 years.

The spectrum is intriguing because it agrees so well at large-scales with Charney's theory of geostrophic turbulence [4], but deviates from that prediction where it shallows. Moreover, the fact that the small-scale slope is $-5/3$ invites multiple explanations, since that is the theoretical slope both for the forward cascade of energy in isotropic, three-dimensional turbulence, and for the inverse cascade of two-dimensional turbulence, as well as other systems. At the large-scale, Charney argued, rotation and stratification conspire to make the atmosphere quasi-two-dimensional. Stirring by baroclinic instability (or any planetary mechanism) will induce a forward cascade of potential enstrophy, reflected in a -3 kinetic energy spectrum below the stirring scale. Moreover, the theory predicts equipartition between kinetic and available potential turbulent energy, and so the temperature variance spectrum should have the same slope as kinetic energy, just as observed. The forward enstrophy cascade in this theory should proceed down to scales at which rotation becomes less important, where unbalanced motions and instabilities might efficiently lead to dissipation. In the atmosphere, a reasonable estimate puts this scale an order of magnitude smaller than the observed transition scale.

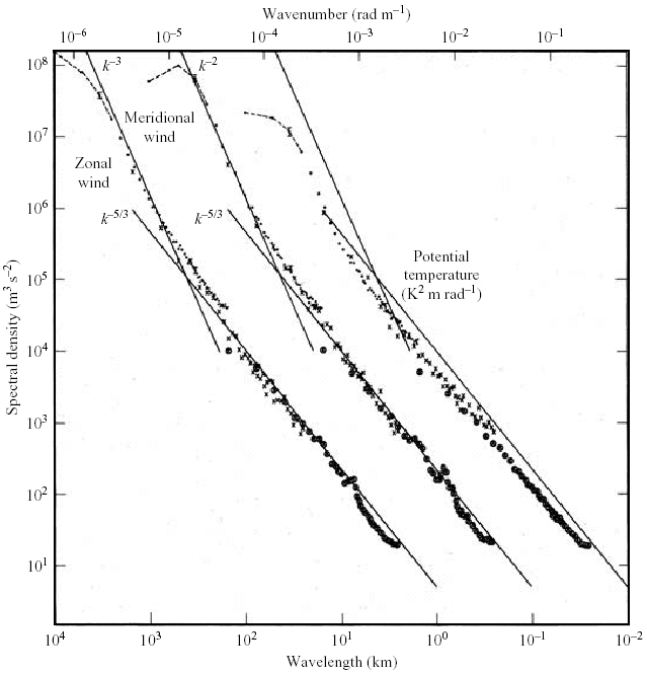

Figure 1: Variance power spectra of horizontal wind and potential temperature near the tropopause from GASP aircraft data, reproduced from ref. 3. The spectra for meridional wind and temperature are shifted one and two decades to the right; lines with slopes -3 and -5/3 are drawn for reference.

Previous explanations

Explanations in the literature for the mesoscale spectrum fall

into three general categories: (*i*) an inverse cascade of small-scale energy, produced perhaps by convection [5–7]; (*ii*) production of gravity waves by divergent flows [8–12]; or (*iii*) a direct cascade of energy from the large-scales [13–16]. More recent observations and analysis present new facts that must be accommodated by theory. Regarding type-(*i*) theories, Cho and Lindborg [17] analyze horizontal velocity data from a series of thousands of fights in the late 1990s at altitudes between 9 and 12 km. From this they infer a forward cascade of energy for scales of order 100 km and smaller. Regarding the hypotheses of type (*ii*), data collected on scales between 1 and 100 km over the Pacific Ocean (the Pacific Exploratory Mission, ref. 18) indicate that mesoscale energy away from the equator is dominated by vortical modes rather than divergent ones [19]. It is pointed out that observations over land may reveal more gravity wave energy at these scales than over the ocean, but even so, a complete theory cannot then rely solely on gravity waves to produce the mesoscale spectrum. In sum, the current state of observational evidence leaves only theories of type (*iii*) as plausible universal explanations of the NG85 data.

Tung and Orlando [13, hereafter TO03] propose a model that, at first glance, explains the observations. The basis of their argument is that the standard model of geostrophic turbulence proposed by Charney is incomplete, because in any finite-width inertial range, there will always be some leakage of energy to small scales [20, 21]. In their theory the subdominant $k^{-5/3}$ cascade reveals itself at the wavenumbers where the direct cascading energy spectra exceeds that of the enstrophy cascade, namely for wavenumbers $k > (\eta/\varepsilon)^{1/2}$, where ε is the downscale energy flux and η is the enstrophy flux. TO03 support their theory with a small number of simulations using a standard numerical two-layer quasigeostrophic forced by baroclinic instability. One of the present authors, however, noted that because the forward energy cascade rate ε depends on the dissipation scale, the transition scale of TO03 will always coincide with the effective Kolmogorov scale of the dissipation mechanism, and so changes with filter strength and grid resolution [22]. A similar spectra to that found by TO03 can be obtained by under-dissipating the forward enstrophy cascade, causing a buildup of enstrophy at the grid scale. In order for the theory of TO03 to be correct, then, the atmosphere must possess a mechanism that selectively dissipates the forward cascade at some fixed O(1 km) scale, independent of energy flux.

The compelling part of the TO03 argument is that the proposed mechanism relies on a forward cascade of vortical energy. An improved theory should also possess that characteristic. Lindborg [14, 15] demonstrates that a forward $-5/3$ slope energy cascade can arise in highly stratified three-dimensional turbulence when rotation is sufficiently weak, though no explicit connection to the synoptic scale is included in this theory. Kitamura and Matsuda [16] do find that such a mechanism seems to arise in a very high resolution non-hydrostatic Boussinesq model, and follows on the tails of a steep synoptic-scale spectrum. But in this case, much as seen by Koshyk, Hamilton and collaborators [12, 23], the energy in the mesoscale spectrum is due to divergent motions. The latter fact is not consistent with the observations of Cho and collaborators [19].

Idealized tropopause dynamics

The GASP observations were collected primarily near the tropopause, the boundary between the well-mixed, low-potential vorticity troposphere and the more stratified, high-potential vorticity stratosphere [24, 25]. Juckes [24] points out that when temperature anomalies of the tropopause and ground are in phase the flow has a structure associated with barotropic flow, and also suggests that tropopause anomalies likely dominate tropospheric potential vorticity anomalies. (This viewpoint is closely related to the Eady model of baroclinic instability [26], in which the tropopause interacts with a similar layer in the lower troposphere to produce baroclinic instability.) Juckes estimates from observations that neglecting tropospheric potential vorticity anomalies will result in an error on the order of 20%. The model he proposes takes into account that the Ertel potential vorticity of the troposphere is nearly constant, and so the balanced dynamics arise primarily from the advection of tropopause temperature.

An idealization of this situation in which the depth of the interior fluid is assumed semi-infinite and the stratification assumed constant is termed 'surface quasigeostrophy' (SQG). This model was first proposed by Blumen (27, but see also 28–30) as a counterpoint to Charney's theory, which explicitly assumes that boundary effects are negligible. By contrast, in SQG boundary advection determines the flow. The SQG equations are,

$$\partial_t \theta + J(\psi,\theta) = 0, \quad z = 0 \qquad (1\text{a})$$

$$\theta = \partial_z \psi \qquad (1\text{b})$$

$$q \equiv \left(\partial_{xx} + \partial_{yy} + \partial_z \sigma^{-2} \partial_z\right)\psi = 0, \quad z < 0 \qquad (1\text{c})$$

$$\psi \to 0 \ \text{ as } \ z \to -\infty \qquad (1\text{d})$$

where ψ is the horizontal streamfunction, $J(\ ,\ )$ is the horizontal Jacobian and $\sigma = N/f$ is Prandtl's ratio (in general N is a function of z, but here we will take it to be a constant). Fourier decomposition in the horizontal plane at $z = 0$ leads to the separable solution

$$\hat{\psi}(\mathbf{k},z) = (\sigma k)^{-1}\, \mathrm{e}^{\sigma k z}\, \hat{\theta}(\mathbf{k},0) \qquad (2)$$

where $k = |\mathbf{k}|$ is the modulus of the horizontal wave-vector $\mathbf{k}$ and the hatted variables are spectral amplitudes. The flow is thus governed by the two-dimensional dynamics at the boundary, where

$$\hat{\psi}(\mathbf{k},0) = (\sigma k)^{-1}\, \hat{\theta}(\mathbf{k},0),$$

yet the resulting flow is three-dimensional.

The turbulent dynamics of SQG differ from those of quasigeostrophic turbulence because the conserved invariants of the system are distinct. In quasigeostrophic dynamics, the conserved invariants are the total energy $E = -\langle \psi q \rangle/2$ and the potential enstrophy $Z = \langle q^2 \rangle/2$, where $\langle\rangle$ represents a volume average. In SQG the invariants are the temperature variance $T = \overline{\theta^2}/2$ and the total energy $E_S = \overline{\psi\theta}/2$, where the overline implies an area average at $z = 0$. [1]

Defining spectral densities such that $E_S = \int \mathscr{E}_S(k)\, dk$ and $T = \int \mathscr{T}(k)\, dk$, the SQG invariants are related as $\mathscr{T} = \sigma k\, \mathscr{E}_S$. In the inverse cascade of total SQG energy, the densities have spectra $\mathscr{E}_S \propto k^{-2}$ and $\mathscr{T} \propto k^{-1}$, while in the forward cascade of temperature variance one has $\mathscr{E}_S \propto k^{-8/3}$ and $\mathscr{T} \propto k^{-5/3}$ [27, 29].

A new model

The fundamental model we propose here is a variant of SQG that highlights the transition between quasi-two-dimensional barotropic flow and baroclinic three-dimensional flow. From the solution connecting ψ and θ (**2**), one sees that as the horizontal scale gets larger (or k gets smaller), the penetration depth of the temperature anomalies increases proportionally, with aspect ratio given by the Prandtl ratio, $\sigma = N/f$. At large enough scale, the penetration will reach deep into the troposphere and interact with the interior flow, if it ceases to be homogenized at some depth, or the lower boundary as an upper limit. The simplest possible extension of SQG that takes this effect into account is the restriction of the domain in (**1**) to a finite depth — specifically, replacing (**1**d) with the condition $\theta = 0$ at $z = -H$. In this case, the replacement of solution (**2**) is

$$\hat{\psi}(\mathbf{k}, z) = \left[\frac{\cosh[\sigma(z+H)\, k]}{\sigma k\, \sinh(\sigma H\, k)} \right] \hat{\theta}(\mathbf{k}, 0), \qquad (\mathbf{3})$$

which at the upper surface becomes

$$\hat{\psi}(\mathbf{k}, 0) = \left[\sigma k\, \tanh(\sigma H\, k) \right]^{-1} \hat{\theta}(\mathbf{k}, 0). \qquad (\mathbf{4})$$

The remarkable property of this finite-depth surface-quasigeostrophic model (fSQG) results from the properties of the hyperbolic tangent in the inversion. At large scales, or $k \ll (\sigma H)^{-1}$, the temperature is related to the streamfunction like $\hat{\theta}(\mathbf{k}, 0) \simeq \sigma^2 H\, k^2\, \hat{\psi}(\mathbf{k}, 0)$, while at small scales, or $k \gg (\sigma H)^{-1}$, the inversion is approximately $\hat{\theta}(\mathbf{k}, 0) \simeq \sigma k\, \hat{\psi}(\mathbf{k}, 0)$. Thus the relation at the surface of streamfunction to advected quantity (temperature) transitions from a QG/2D-like inversion at large scales, to an SQG-like inversion at small scales, with the transition occurring at the wavenumber

$$k_t \equiv (\sigma H)^{-1} = \frac{f}{NH}. \qquad (\mathbf{5})$$

Note that this predicted transition scale is only equal to the deformation scale when H is taken as the full depth of the troposphere, which we take as an upper bound. This will be considered further in the discussion.

The spectral slopes can be predicted as follows. Defining the spectral density of the streamfunction by the relation $\overline{\psi^2}/2 = \int \mathscr{P}(k)\, dk$, the conserved invariants have the form

$$\mathscr{E}_S(k) = \sigma k\, \tanh(k/k_t)\, \mathscr{P}(k) \qquad (\mathbf{6}\text{a})$$

$$\mathscr{T}(k) = \left[\sigma k\, \tanh(k/k_t) \right]^2 \mathscr{P}(k) \qquad (\mathbf{6}\text{b})$$

In the present context we are interested in the influence synoptic-scale stirring on the mesoscales, presumably due to baroclinic instability, and so we restrict our attention to the forward cascade regime, in which the conservation of temperature variance determines the spectrum via the standard phenomenology [31, 32]. The temperature variance spectrum (**6**b) has the same dimensions as kinetic energy, and so it is the flux of this boundary-flow energy that is constant in its inertial range,

$$\varepsilon \simeq k \mathscr{T}(k) \tau^{-1}(k) = \text{constant} \qquad (\mathbf{7})$$

where $\tau(k)$ is the turbulent timescale at wavenumber k. Since the turbulent timescale is the advective timescale, we can express it in terms of the streamfunction spectrum, $\tau(k) \simeq \left[k^5 \mathscr{P}(k) \right]^{-1/2}$. Using this expression in (**7**) and eliminating $\mathscr{P}(k)$ with the help of (**6**b) reveals that

$$\mathscr{T}(k) = C_T \varepsilon^{2/3} \left[\sigma\, \tanh(\sigma H\, k) \right]^{2/3} k^{-5/3}, \qquad (\mathbf{8})$$

where C_T is the appropriate Kolmogorov constant.

It is the temperature variance spectrum that determines all other spectra in the direct cascade range, and so, for example, we can derive $\mathscr{P}(k)$ via elimination of $\mathscr{T}(k)$ between (**6**b) and (**8**), and similarly for $\mathscr{E}_S(k)$. More to the point, the kinetic energy spectrum is

$$k^2 \mathscr{P}(k) = \left[\sigma \tanh(\sigma H\, k) \right]^{-2} \mathscr{T}(k), \qquad (\mathbf{9})$$

which thus takes on the small- and large-scale limits

$$k^2 \mathscr{P}(k) \simeq \begin{cases} C_T \varepsilon^{2/3} (\sigma^2 H)^{-4/3}\ k^{-3}, & k \ll k_t \\ C_T \varepsilon^{2/3} \sigma^{-4/3}\ k^{-5/3}, & k \gg k_t \end{cases} \qquad (\mathbf{10})$$

To summarize, the hypothesis is that synoptic scale stirring produces a balanced, forward cascade of temperature variance at the tropopause (and perhaps at the ground as well).

[1] The invariant E_S is proportional to the total energy of the flow; multiplying the potential vorticity q by $-\psi$ and integrating over volume, one has that

$$\langle |\nabla\psi|^2 + \sigma^{-2}\, \theta^2 \rangle = \sigma^{-2} H_a^{-1}\, \overline{\psi\theta}\Big|_{z=0} - \langle \psi q \rangle,$$

which is just twice the total energy E (here H_a is some averaging depth). Thus if $q \equiv 0$ the total energy is $E = (1/2)\sigma^{-2} H_a^{-1}\, \overline{\psi\theta} = \sigma^{-2} H_a^{-1} E_S$.

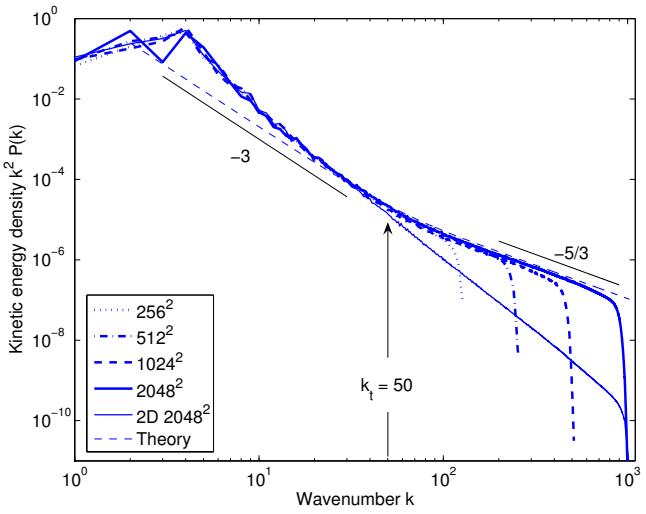

Figure 2: Finite depth SQG kinetic energy spectra at $z = 0$ with $k_t = 50$, computed at different horizontal resolutions. The thin solid line shows a calculation of regular two-dimensional turbulence for reference, and the thin dashed line is the theoretical spectrum (**9**), with constant chosen to match the large scale spectra.

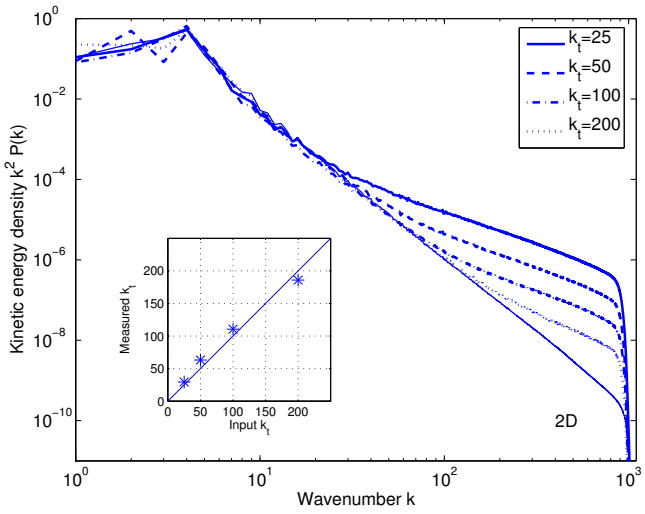

Figure 3: Finite-depth SQG kinetic energy spectra $k^2\mathscr{P}(k)$ at $z = 0$ with $k_t = 25$, 50, 100, and 200 at 2048^2 resolution. The thin solid line is the spectrum from a simulation of standard two-dimensional turbulence, shown for reference. The inset plot shows the measured transition wavenumber compared to the input value k_t. See text for details.

At large scales, the flow is quasi-barotropic because the penetration depth is large enough to interact with the interior flow (or the lower boundary as an upper limit), and here the cascade exhibits the same kinetic energy spectrum as in Charney's theory of quasigeostrophic turbulence. As the cascade proceeds, the penetration depth of temperature anomalies decreases. When the vertical scale is small compared to the depth over which the tropospheric interior potential vorticity is homogenized, the cascade flattens to a $-5/3$ slope, recovering its essential SQG-like nature. The accompanying temperature spectrum is considered in the discussion.

Numerical tests of the predicted spectra

Here we present the results of a series of simulations of the fSQG model, forced by large-scale stirring and dissipated scale-selectively at both the domain and grid scales. The system modeled is just (**1**a) with added forcing and dissipation terms, coupled with the $\hat{\psi}$-$\hat{\theta}$ inversion for the finite-depth model (**4**). The calculation is performed in the spectral domain, corresponding to a 2π-periodic physical domain, using a de-aliased fast Fourier transform method to calculate the non-linear terms, via the staggered grid method of Orszag [33]. Stirring is generated at $k_f = 4$ by a random Markovian process that is highly correlated in time (so that the decorrelation time is longer than the eddy turnover time in the cascade). Large-scale dissipation of the inverse cascade is accomplished with a strong linear drag on temperature. The forward cascade of temperature variance is dissipated using a highly scale-selective exponential cutoff. The filter is explicitly restricted to act only on $k \gtrsim 2k_{\max}/3$, but in fact affects a much smaller range of wavenumbers close to $k_{\max}$. The details of the filter are discussed in ref. 22. In all cases, the filter is sufficiently strong that the high-wavenumber spectrum is minimally influenced by the filter, but strong enough to ensure our effective Kolmogorov scale is resolved.

Figure 2 shows a plot of the kinetic energy spectra $k^2\mathscr{P}(k)$ for a series of simulations performed at resolutions ranging from 256^2 ($k_{\max} = 127$) to 2048^2 ($k_{\max} = 1023$), all using $\sigma = 1$ and $H = 1/50$, so that the input transition wavenumber is $k_t = 50$. Also shown for reference is the result of a simulation of standard two-dimensional Euler (TDE) turbulence, forced and dissipated identically to the other runs, performed at 2048^2 resolution, and the theoretical spectrum (**9**), with constant chosen to match the large scale spectra. The small-scale filter is adjusted for each simulation so that it acts only near the highest resolved wavenumber, as explained above. Each spectrum was calculated by averaging over time (for the portion of the simulation over which the flow was in steady state) and azimuthal angle in the horizontal plane.

At large scales, all fSQG spectra follow the TDE spectra. That said, all are steeper than a -3 slope near the forcing scale, but this is not uncommon for the direct cascade range in two-dimensional turbulence. The consistency at large-scales between the fSQG and TDE simulations indicate that deviations from -3 at wavenumbers near the forcing scale reflect the forcing mechanism and intrinsic dynamics of forced two-dimensional turbulence with drag, not the intrinsic dynamics of the fSQG model. The shallow slope for all fSQG runs at $k > k_t$ approaches $-5/3$, as expected. Crucially, the series of simulations represented in figure 2 shows that the transition

scale is independent of resolution and small-scale dissipation.

In order to check that the transition scale that arises from the simulation is truly proportional to the input transition wavenumber k_t, we performed a series of simulations at 2048^2 resolution, with k_t equal, respectively, to 25, 50, 100, and 200 ($\sigma = 1$ for all simulations, and H was varied). The energy generation rate was normalized by $(\sigma^2 H)^{-1}$ for each simulation[2]. Figure 3 shows the kinetic energy spectra for each run, along with the spectra from a simulation of standard two-dimensional turbulence for comparison. One can see that the resulting transition wavenumber increases with increasing input k_t. The inset axes in figure 3 shows the measured estimates of the transition wavenumber plotted against the input parameter, k_t (the measured transition wavenumber is defined as the wavenumber where the spectral slope is $k^{-15/6}$). The plot indicates that the transition wavenumber is well-approximated by f/NH, as expected.

Discussion

The proposed model for the effects of tropopause temperature anomalies on the atmospheric energy spectrum should be taken as a heuristic tool, not as a complete theory. The model is significant, however, because it demonstrates how turbulent motions at the synoptic scale can produce a balanced, forward cascade of temperature variance, resulting in an upper-tropospheric spectrum with a break at a scale that is a function of fundamental background parameters. The numerical simulations presented here moreover demonstrate that such a transition indeed occurs in the fSQG model, and that the transition is robust, is well-predicted by the natural scale f/NH, and is independent of both model resolution and small-scale dissipation. Therefore, one need invoke neither unbalanced dynamics nor an inverse cascade to produce the spectra observed in the GASP data.

The form of the predicted transition scale (**5**) implies a distinct geographical dependence. While N is roughly constant throughout the troposphere, f varies with latitude. Also, depending on the interpretations of H, one could argue that the deeper tropical troposphere should translate into a larger tropical homogenization depth. Thus where f increases, H likely decreases, and so the transition scale should decrease with increasing latitude. Figure 8 of NG85, which plots the spectra of wind and temperature as functions of latitude band, indicates that this is the situation.

The model suggested here can explain many features of the observations, but taken on its own has important limitations. Using typical mid-latitude tropospheric values of $N \sim 10^{-2}\mathrm{s}^{-1}$ and $f \sim 10^{-4}\mathrm{s}^{-1}$, the predicted transition scale between the two slopes is $L_t = NH/f \sim 100\ H$. Therefore a transition scale on order hundreds of kilometers, as observed by NG85, requires a vertical scale on order kilometers. This is consistent with the notion of the tropospheric depth as an upper bound on H, with such a bound occurring in the limit that potential vorticity is assumed constant throughout the entire thickness of the troposphere. However, if we take $H = H_{\text{troposphere}}$, then the transition wavenumber (**5**) is equivalent to the Rossby deformation wavenumber. If baroclinic instability induces the cascade of temperature variance, one then must have $H < H_{\text{troposphere}}$ in order for a -3 cascade range to exist. The most straightforward way to include baroclinic instability in the present model is to replace the lower isothermal boundary condition with a second active temperature layer [34], but in this case it is not clear that the transition scale will be different than in our one-layer finite-depth model. One might also question the assumption of constant tropospheric and infinite stratospheric stratification. Following Juckes [24], it is straightforward to show that adding a stratospheric layer changes the large scale spectral slope, but also does not alter the expected transition scale[3]

Another issue not yet addressed is the vertical structure of the spectra. If the entire troposphere were truly dominated by the dynamics of temperature advection at the tropopause, then at scales smaller than the transition scale, one should see an evanescently decaying signal as one moves down into the troposphere. Tracer spectra should also, in this case, show qualitatively different behavior at depth than at the tropopause [35]. Gao and Meriwether [36] present an analysis of a limited set of data taken at 6 km, and not unexpectedly, there is energy at mesoscale mid-depths. They do find that the spectrum of energy is steeper (close to -2) than that of the GASP data, but there is more amplitude than would be expected from purely tropopause-trapped flow.

Finally, careful consideration of the predicted fSQG spectra indicates a potential inconsistency between the present theory and the NG85 potential energy spectrum $\sigma^{-2}\mathscr{T}(k)$. The potential energy spectrum predicted at large scales by the fSQG model is shallower than that predicted by the Charney theory, while the data of NG85 indicate equipartition at all scales, consistent with Charney's theory. Using (**9**) the ratio of potential to kinetic energy in fSQG is

$$\frac{\sigma^{-2}\mathscr{T}(k)}{k^2\mathscr{P}(k)} = [\tanh(\sigma H\, k)]^2.$$

At $k \ll k_t$, potential energy thus has a slope of approximately k^{-1}, but is smaller than the kinetic energy by the ratio $(k/k_t)^2$, while at $k \gg k_t$, fSQG predicts equipartition.

[2] A unit input of θ scaled by $(\sigma^2 H)^{-1}$ will result in the same streamfunction as a unit input of two-dimensional vorticity, because $(\sigma^2 H)^{-1}$ is the factor in the $\hat{\theta} \to \hat{\psi}$ inversion at large scale, where the energy is injected.

[3] Assuming a stratospheric buoyancy frequency N_s and a tropospheric buoyancy frequency N_t, and retaining the isothermal condition at the ground, the connection between streamfunction and potential temperature at the tropopause (**4**) changes to

$$\hat{\psi}(\mathbf{k},0) = \frac{1-r^2}{\sigma k\ [\tanh(\sigma H\, k)+r]}\ \hat{\theta}(\mathbf{k},0).$$

where $\sigma = N_t/f$ is the tropospheric Prandtl ratio and $r = N_t/N_s$.

The three inadequacies of the present model noted in the previous few paragraphs can be resolved with a simple extension. If both surface and interior anomalies are active in generating the flow, then interior dynamics should dominate the temperature spectrum at large scales, and so large-scale available potential and kinetic energy will be in equipartition, as observed. At scales smaller than the transition scale, fSQG predicts equipartition between potential and kinetic energy, but also predicts that both will have spectra that are shallower and of larger amplitude than those generated by the interior flow. Thus at small scales the energy generated by the surface-trapped cascade will emerge to dominate the spectra of both kinetic and potential energy (Held et al. [30] make a similar hypothesis in their conclusion). Moreover, the emergence of the $-5/3$ surface-trapped cascade may occur at smaller scales than k_t when the large scales are dominated by the -3 interior dynamics, depending on the relative strength of the surface and interior forcing.

It may be the case that a continuously stratified quasi-geostrophic model in which both lower and upper boundary temperature advection are explicitly taken into account (isothermal boundaries are used in most numerical quasi-geostrophic models) would reveal a spectral signature quantitatively similar to that observed by NG85. This, as well as other details of the problem will be considered in a forthcoming paper. Nevertheless, the consistency of the predictions for the observed *mesoscale* spectrum with or without significant interior flow anomalies is a satisfying feature of the simple model suggested here.

The authors thank Oliver Bühler, Isaac Held, Martin Juckes, Guillaume Lapeyre, Andrew Majda, Tapio Schneider and an anonymous reviewer for constructive comments on this work. Both authors were supported by the National Science Foundation under grant OCE-0327470. The numerical calculations were performed using NYU's new high performance computational cluster, Max.

1. Nastrom, G. D. & Gage, K. S. (1985) *J. Atmos. Sci.* **42**, 950–960.
2. Perkins, P. J. (1976) *NASA-TMX-73544*.
3. Nastrom, G. D., Gage, K. S. & Jasperson, W. H. (1984) *Nature* **310**, 36–38.
4. Charney, J. G. (1971) *J. Atmos. Sci.* **28**, 1087–1095.
5. Gage, K. S. (1979) *J. Atmos. Sci.* **36**, 1950–1954.
6. Lilly, D. K. (1989) *J. Atmos. Sci.* **45**, 2026–2030.
7. Vallis, G. K., Shutts, G. J. & Gray, M. E. (1997) *Quart. J. Roy. Meteor. Soc.* **123**, 1621–1652.
8. DeWan, E. M. (1979) *Science* **204**, 832–835.
9. VanZandt, T. E. (1982) *Geophys. Res. Lett.* **9**, 575–578.
10. Yuan, L. & Hamilton, K. P. (1994) *J. Fluid Mech.* **280**, 369–394.
11. Gardner, C. S., Hostetler, C. A. & Franke, S. J. (1993) *J. Geophys. Res.* **99**, 20,601–20,622.
12. Koshyk, J. N., Hamilton, K. P. & Mahlman, J. D. (1999) *Geophys. Res. Lett.* **26**, 843–946.
13. Tung, K. K. & Orlando, W. W. (2003) *J. Atmos. Sci.* **60**, 824–835.
14. Lindborg, E. (2005) *Geophys. Res. Lett.* **32**, L01809.
15. Lindborg, E. (2006) *J. Fluid Mech.* **550**, 207–242.
16. Kitamura, Y. & Matsuda, Y. (2006) *Geophys. Res. Lett.* **33**, L05809.
17. Cho, J. Y. N. & Lindborg, E. (2001) *J. Geophys. Res.* **106**, 10223–10232.
18. Cho, J. Y. N., Zhu, Y., Newell, R. E., Anderson, B. E., Barrick, J. D., Gregory, G. L., Sachse, G. W., Carroll, M. A. & Albercook, G. M. (1999) *J. Geophys. Res.* **104**, 5697–5716.
19. Cho, J. Y. N., Newell, R. E. & Barrick, J. D. (1999) *J. Geophys. Res.* **104**, 16297–16308.
20. Eyink, G. L. (1996) *Physica D* **91**, 97–142.
21. Tung, K. K. & Welch, W. T. (2001) *J. Atmos. Sci.* **58**, 2009–2012.
22. Smith, K. S. (2004) *J. Atmos. Sci.* **61**, 937–942.
23. Koshyk, J.N. & Hamilton, K. P. (2001) *J. Atmos. Sci.* **58**, 329–348.
24. Juckes, M. N. (1994) *J. Atmos. Sci.* **51**, 2756–2768.
25. Schneider, T. (2004) *J. Atmos. Sci.* **61**, 1317–1340.
26. Eady, E. T. (1949) *Tellus* **1**, 33–52.
27. Blumen, W. (1978) *J. Atmos. Sci.* **35**, 774–783.
28. Hoyer, J.-M. & Sadourny, R. (1982) *J. Atmos. Sci.* **39**, 707–721.
29. Pierrehumbert, R. T., Held, I. M. & Swanson, K. L. (1994) *Chaos, Solitons & Fractals* **4**, 1111–1116.
30. Held, I. M., Pierrehumbert, R. T., Garner, S. T. & Swanson, K. L. (1995) *J. Fluid. Mech.* **282**, 1–20.
31. Kolmogorov, A. N. (1941) *Dokl. Acad. Sci. USSR* **30**, 299–303.
32. Obukhov, A. M. (1941) *Dokl. Akad. Nauk SSSR* **32**, 22–24.
33. Orszag, S. A. (1971) *J. Fluid Mech.* **146**, 21–43.
34. Blumen, W. (1978) *J. Atmos. Sci.* **35**, 784–789.
35. Scott, R. K. (2005) *Phys. Fluids* p. Submitted.
36. Gao, X. & Meriwether, J. W. (1998) *J. Geophys. Res.* **103**, 6397–6404.